Chemical Physics Letters 493 (2010) 333–339

Contents lists available at ScienceDirect

Chemical Physics Letters

journal homepage: www.elsevier.com/locate/cplett

A photochromic thin film based on salicylideneaniline derivatives intercalated layered double hydroxide

Xin Rui Wang, Jun Lu, Dongpeng Yan, Min Wei *, David G. Evans, Xue Duan

State Key Laboratory of Chemical Resource Engineering, Beijing University of Chemical Technology, Beijing 100029, PR China

ARTICLE INFO

Article history:
Received 3 December 2009
In final form 24 May 2010
Available online 31 May 2010

ABSTRACT

Optically transparent thin films with photochromic properties have been fabricated by means of co-intercalation of azomethine-H anions (AMH) and 1-pentanesulfonate (PS) with different molar ratios into the galleries of a ZnAl layered double hydroxide (LDH). The photochromism of AMH occurred in a 2D confined inorganic matrix has been studied by steady state and transient UV–vis spectroscopy. The AMH anion undergoes an excited-state intramolecular proton transfer from the enol tautomer to *trans*-keto tautomer after UV excitation, and the relaxed back-isomerization to the ground state of enol tautomer was investigated by transient UV–vis spectroscopy.

1. Introduction

Light-induced reversible color change of substances is known as photochromism and has attracted considerable attention from various fields of chemistry and materials science [1]. Salicylideneanilines and related Schiff bases, generally called anils, are characterized by a very good fatigue factor and can exhibit photochromism in various states (solution, crystal, rigid glass, and even biological media) [2–5]. After the excitation of the initial enol (*anti*-enol) tautomer, the excited-state intramolecular proton transfer (ESIPT) occurs, leading to the excited keto tautomer (*cis*-keto or its zwitterionic form), exhibiting a characteristic, strongly Stokes fluorescence band. Subsequently, after the structural changes (rotation around C=C and/or C–N bond; see Fig. 1) involving the cleavage of the intramolecular hydrogen bond, the red long-lived photochromic tautomer (*trans*-keto or its zwitterionic form) in the ground state is generated either by thermal treatment or by irradiation of visible light. Recently, many studies on this subject have been carried out and Schiff bases have been widely used in the fields of laser dyes, higher energy radiation detectors, molecular memory storage devices and switches [1,6].

Since photochromism of Schiff base compounds is attributed to geometrical isomerization, it would be sensitive to molecular environment. Maciejewski and co-workers studied the photochromic cycle of salicylaldehyde azine in a number of different solvents and micellar systems [7], and the results showed that the lifetime of *cis*-keto and *trans*-keto tautomer was drastically affected by polarizability, viscosity and protonation of the solvents. From the viewpoint of manipulation and application of Schiff bases however, the modulation of photochromism cycle based on different solvents is not suitable and feasible. Therefore, an effective solution for modulating and enhancing the photochromic properties of salicylideneaniline derivatives is to choose an appropriate solid material as host matrix to tune its molecular micro-environment.

Layered double hydroxides (LDHs), whose structure can be generally expressed as $[M^{II}_{1-x}M^{III}_{x}(OH)_2](A^{n-})_{x/n}\cdot mH_2O$ (where M^{II} are divalent and M^{III} trivalent metals, respectively, and A^{n-} an anion), are 2D layered materials consisting of positively charged host layers with charge balancing guest anions [8–11]. One of the most interesting features of these materials is their role as a host matrix for the orientation and dispersion of interlayer anions, in order to afford tailored optical, thermal and electrical functional materials as well as devices [12–16]. Therefore, it can be anticipated that the incorporation of salicylideneaniline derivatives into an LDH matrix will give rise to one kind of novel photochromic material with the following advantages. Firstly, the LDH host layers provide a rigid and ordered micro-environment for the distribution and alignment of the chromophoric group within the available free space, which should affect the barrier of tautomerization. Secondly, the homogeneous distribution of dye molecules in the solid matrix based on host–guest interactions can avoid dye aggregation and fluorescence quenching effectively. Finally, the presence of the inorganic LDH host matrix may improve the thermal and optical stability of the intercalated organic dye.

In this work, we report the fabrication of transparent thin films of azomethine-H anions (AMH) (shown in Fig. 1) and 1-pentanesulfonate (PS) co-intercalated in LDH matrix, which show photochromic behavior. The employment of PS is to provide the AMH molecule with a homogeneous nonpolar environment so as to prevent its aggregation and thus enhance the photochromism and the photoemission properties. The correlation between AMH luminescence and its concentration was also explored, and the sample with

* Corresponding author. Fax: +86 10 64425385.
E-mail addresses: weimin@mail.buct.edu.cn, weimin-hewei@163.com (M. Wei).

0009-2614/$ - see front matter © 2010 Elsevier B.V. All rights reserved.
doi:10.1016/j.cplett.2010.05.071

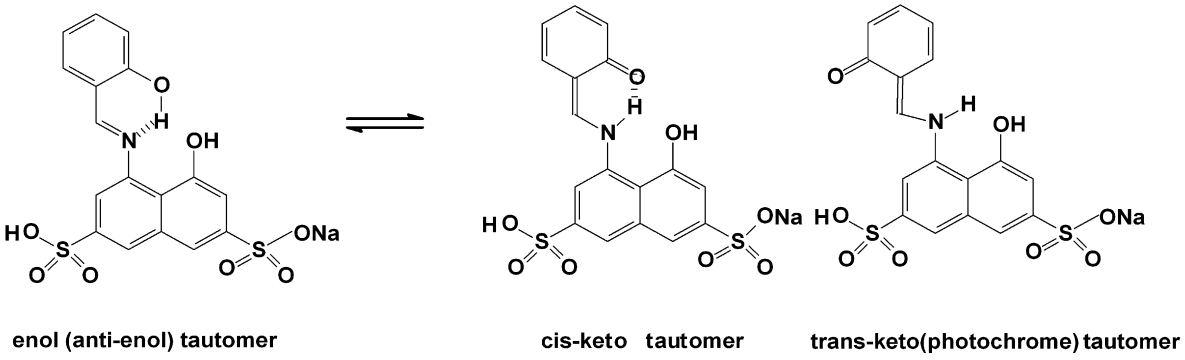

Fig. 1. Tautomeric equilibrium of azomethine-H monosodium salt hydrate (AMH).

2% AMH molar percentage with respect to the total organic guests, exhibits the optimal luminous intensity. Upon UV excitation, AMH undergoes an excited-state intramolecular proton transfer from the enol tautomer to *trans*-keto tautomer, and the relaxed back-isomerization to the ground state of enol tautomer was recorded by transient UV–vis spectroscopy. To the best of our knowledge, there is no previous report on photochromic films ruled by excited-state intramolecular proton transfer of salicylideneaniline derivatives immobilized in an inorganic matrix. It is expected that the strategy reported in this work can be employed to fabricate a variety of film materials with interesting photochromic properties based on regular arrangements of organic chromophores within a 2D inorganic matrix.

2. Experimental section

The AMH/PS-LDH composite was synthesized using a method involving separate nucleation and aging steps (SNAS) developed in our laboratory [17]. The matched molar ratio of Zn^{2+}/Al^{3+} was 2.0 in this work. The AMH molar percentage with respect to the total organic guests changed from 0.1% to 100%, and more detail could be seen in Supplmentary material. Thin films of AMH/PS-LDH were fabricated by the solvent evaporation method. The AMH/PS-LDH powder (0.01 g) was suspended in ethanol (20 mL) in a glass flask and treated in an ultrasonic bath in N_2 atmosphere for 15 min. After filtration using a membrane filter (0.2 μm, Millipore), 5 mL of AMH/PS-LDH ethanol suspension was dropped onto quartz substrates and dried in vacuum at ambient temperature for 5 h.

Powder X-ray diffraction (PXRD) patterns were obtained using a Shimadzu XRD-6000 diffractometer under the following conditions: Cu Kα radiation (λ = 1.541844 Å, 2θ = 2–70°), 40 kV, 30 mA. CHN analysis was conducted using an Elementar vario elemental analyzer. The content of Zn and Al were analyzed with a Shimadzu ICPS-7500 instrument. The morphology of AMH/PS-LDH thin film was investigated by using a scanning electron microscope (SEM Hitachi S-3500). The stationary UV/vis absorption spectra were measured with a UV/visible absorption spectrophotometer (Shimadzu UV-2100S). The fluorescence emission spectra were recorded on a RF-5301PC fluorospectrophotometer and the width of both the excitation and emission slit is 3 nm.

The time-resolved emission measurements (time correlated single photon counting) were carried out on a LifeSpec-red lifetime spectrometer (Edinburgh Instruments Ltd., UK) equipped with an emission double monochromator and a time resolution of 25 ps after deconvolution of the excitation pulse. From the recorded fluorescence decay curves, the percentage contribution of each lifetime component to the total decay was calculated with the F900 Edinburgh instruments software. The fluorescence decay curves were analyzed with excitation wavelength of 360 nm and observation wavelength of 418, 418, 441, 493, 493, 493 nm for AMH solution, 2%, 10%, 50%, 75%, 100% AMH-LDH thin film, respectively.

Laser flash photolysis experiments were carried out using an Edinburgh LP920 spectrophotometer (Edinburgh Instruments) to record the transient absorption spectra. Sample was excited using 355 nm output with pulse energies of 1.5 mJ/pulse from an OPO pumped by a Nd:YAG laser (10 Hz, 8 ns) (Continuum Surelite). Data were analyzed by the online software of the LP920 spectrophotometer. The fitting quality was judged by weighted residuals and a reduced χ^2 value.

3. Results and discussion

3.1. Crystal structure and composition of AMH/PS-LDH films

Fig. 2A shows the XRD patterns of AMH and PS co-intercalated LDH samples *x* % AMH-LDH, in which *x* % stands for the initial molar percentage of AMH accounting for the summation of AMH and PS. In each case, the XRD pattern exhibits the characteristic reflections of the LDH structure with a series of 0 0 *l* peaks appearing as narrow, symmetric, strong lines at low angle. The absence of any non-basal reflections (h, $k \neq 0$) at high angle for the films is as expected for extremely well *c*-oriented assemblies of LDH platelets [18]. All the patterns of these samples can be indexed to a hexagonal lattice. It can be observed from Fig. 2B that the interlayer spacing ($d_{0\,0\,3}$) of AMH/PS-LDH films decreases from 16.62 Å (x = 0) to the minimum (15.02 Å, x = 100), indicating that AMH and PS were co-intercalated in the galleries of LDH. The variation of the interlayer spacing can be attributed to the different arrangements of interlayer guest molecules with different ratios of AMH/PS. The FT-IR spectra further confirmed the co-intercalation of the two anions (Fig. S1): upon increasing *x* value, the relative intensity of the antisymmetric and symmetric CH2 stretching vibration bands at 2951 and 2861 cm^{-1} decreases (in PS anions); while the relative intensity of the C=N band at 1621 cm^{-1} increases (in AMH anions) [19,20]. The product compositions corresponding to different initial nominal contents are given in Table S1. It can be seen that the experimental ratio of AMH to PS in the materials of AMH/PS-LDH is close to the initial nominal ratio as expected.

Thermolysis behavior of both pristine and intercalated AMH was studied. As shown in Fig. S2, DTA of the pristine AMH shows two exothermic peaks at 429 and 519 °C, which can be attributed to thermal decomposition of the organic material. After intercalation of AMH into the LDH host, the thermal decomposition characteristics of the resulting product are significantly different. Dehydroxylation of the LDH layers overlaps with thermal degradation of the AMH anions and the DTA curve shows two exothermic peaks at 461 and 529 °C, respectively. The results suggest that the

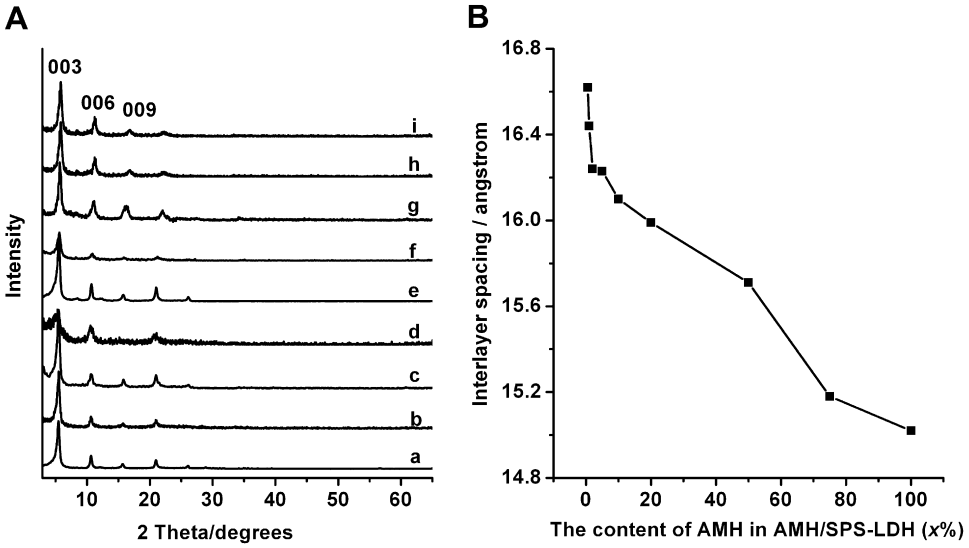

Fig. 2. (A) Powder XRD patterns of the AMH/PS-LDH (*x* %) samples: (a) 0.5%, (b) 1%, (c) 2%, (d) 5%, (e) 10%, (f) 20%, (g) 50%, (h) 75% and (i) 100%. (B) The plot of interlayer spacing *vs.* AMH concentration.

thermal stability of AMH is enhanced by intercalation into the galleries of LDH.

3.2. Surface morphology of AMH/PS-LDH films

SEM images of the 2% AMH-LDH film are shown in Fig. 3, since it exhibits superior photoemission behavior and the longest fluorescence lifetime, which will be discussed in the next section. It was found that the film shows a flat surface in the top view (Fig. 3A and B), with the individual LDH platelets (diameter of *ca.* 200 nm) densely packed in the film plane. A high degree of *c*-axis orientation of the LDH platelets was observed, and the face-to-face stacking of platelets is predominant in the LDH film, consistent with the XRD result (Fig. 2). The side view image (Fig. 3C) reveals that the thickness of the film is about 2.1–2.4 μm with anisotropic structure.

3.3. Optical properties of pristine AMH in solution

The pristine AMH in water solution used as the isotropic system was studied firstly, for the purpose of understanding the photoproperties of the intercalated AMH in LDH gallery.

3.3.1. Steady state absorption and fluorescence spectra

The steady state absorption and fluorescence (emission and excitation) spectra are shown in Fig. 4. The absorption spectrum (Fig. 4A) presents maximal absorption band centered at *ca.* 356 nm (the split is attributed to the vibrational fine structure of the naphthyl in AMH), which originates from the transition $S_0 \rightarrow S_1$ (π, π^*) of the primary enol tautomer, in agreement with the literature [21]. It has been reported that in the absorption spectra of other photochromic Schiff bases, an additional long-wavelength band was observed in protic solvents ascribed to the $S_0 \rightarrow S_1$ (π, π^*) transition of the *cis*-keto tautomer stabilized by intermolecular hydrogen bond [22,23]. For AMH however, no indication of such band was found even in water, indicating that the enol tautomer is more stable than the *cis*-keto tautomer in the free state. This can also be confirmed by fluorescence spectrum (Fig. 4B). The dominant signal at $\lambda = 418$ nm is due to the emission from the primary excited enol tautomer, while the long-wavelength emission with the characteristic large Stokes' shift from the *cis*-keto tautomer cannot be detected in water solution. However, dual emission (enol at 430 and *cis*-keto at 500 nm) was detected in chloroform solution, indicating the quenching effect of polar solvent on the emission of *cis*-keto form (as shown in Fig. S3 and the associated discussion). The fluorescence excitation spectrum agrees well with the UV–vis absorption spectrum. The good 'mirror image' relationship between absorption and fluorescence excitation spectra was observed, indicative of the identity of the absorbing and fluorescent species. AMH in water solution was studied by detecting its fluorescence decays with excitation and emission wavelength of 360 and 418 nm, respectively. The fluorescence lifetime of 2.61 ns was obtained by fitting the decay profiles with one exponential form (as shown in Fig. S4 and Table 1).

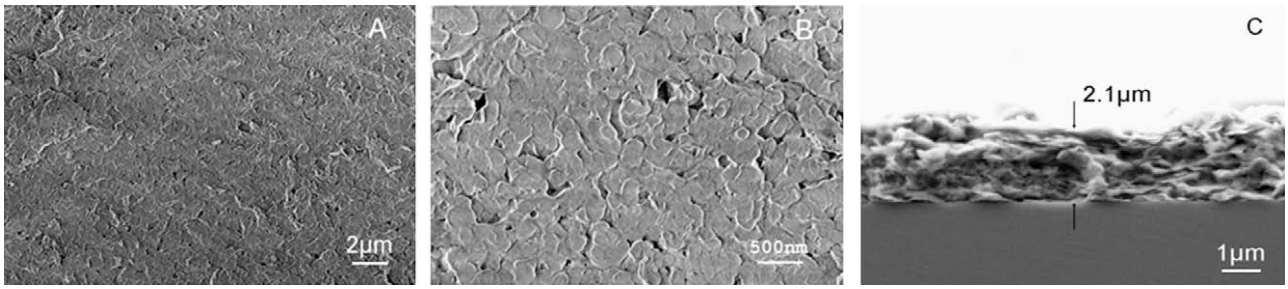

Fig. 3. SEM images of the 2% AMH-LDH film for top view at (A) low and (B) high magnification; (C) the side view image.

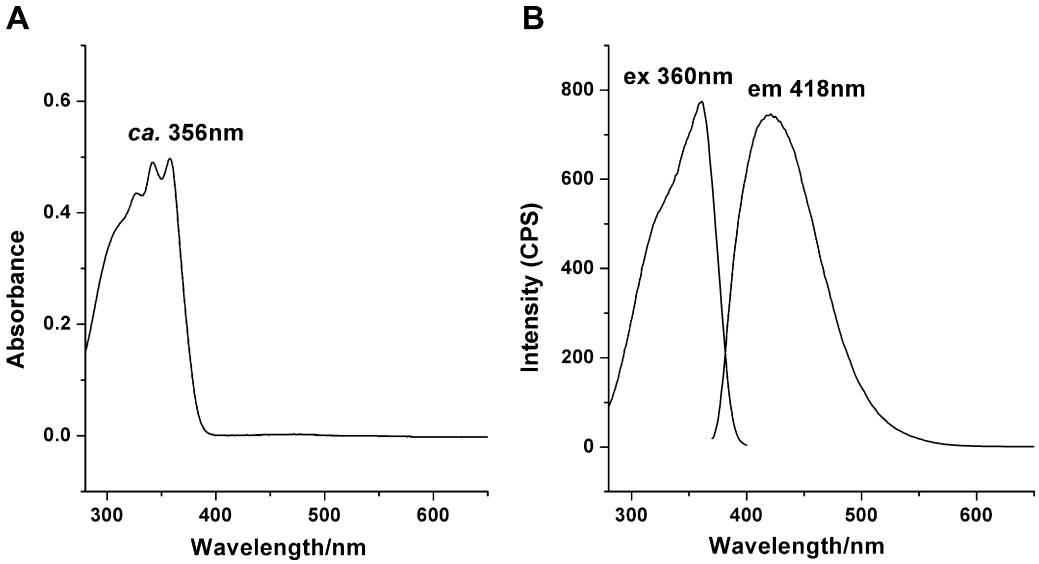

Fig. 4. (A) The steady state absorption spectrum; (B) the fluorescence emission and excitation spectra of pristine AMH in water solution (5×10^{-5} mol/L).

Table 1
Fluorescence decay data of AMH in solution and the AMH/PS-LDH film samples.

x (%)	τ_i (ns)	A_i (%)	$\langle\tau\rangle$ (ns)	χ^2
2	18.92 1.16	87.43 12.57	16.69	1.15
10	18.63 2.97	80.47 19.53	15.57	1.40
50	18.41 2.31	79.47 20.53	15.10	1.45
75	16.95 2.87	66.23 33.77	12.20	1.31
Solution/5×10^{-5} M	2.61	100	2.61	1.08

τ is the fluorescence lifetime; $\langle\tau\rangle$ is the intensity average lifetime; A_i is the intensity of ith component of time constant τ_i. The goodness of fit is indicated by the value of χ^2.

3.3.2. Time-dependent UV/vis absorption spectra

The UV/vis absorption spectra of pristine AMH in water solution (5.0×10^{-5} M) were recorded after UV light irradiation for 0, 60 and 180 s, respectively (Fig. S5). A new band ranging in 450–600 nm appears and increases along with UV irradiation. This is consistent with previous report that the enol-form can tautomerize to the keto-form upon UV irradiation for the photochromism of Schiff base [24–26].

3.3.3. Transient absorption spectra

Fig. 5 shows the transient absorption spectra of the AMH (5.0×10^{-5} M) solution in nitrogen-saturated water after laser flash photolysis at 355 nm. The transient absorption spectra can be distinguished as follows: firstly, the three weak negative bands below 360 nm are due to ground state of the initial enol tautomer, corresponding well to the steady state absorption spectrum (Fig. 4A); secondly, the positive band with a maximum at

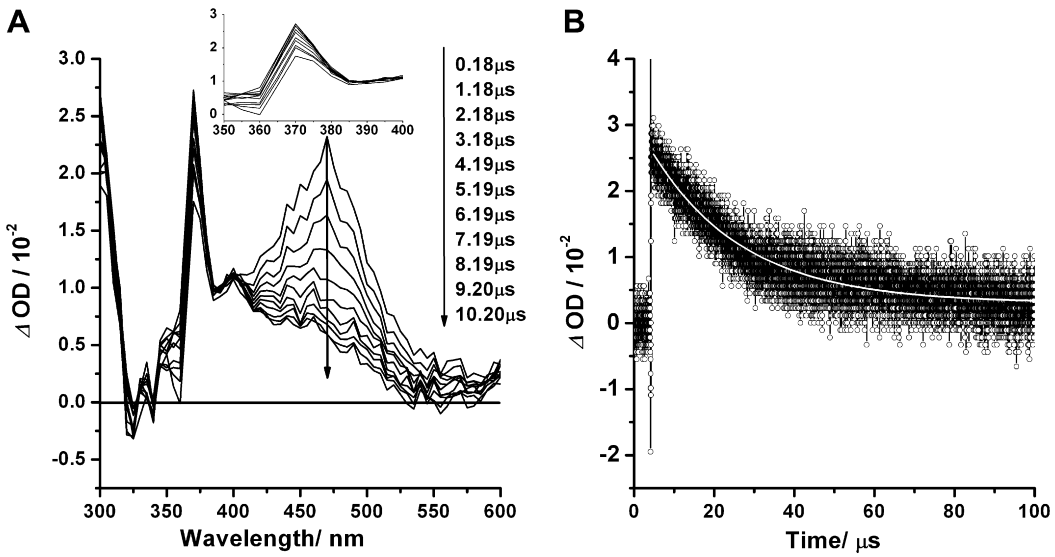

Fig. 5. (A) Transient absorption spectra observed by laser photolysis of nitrogen-saturated solution of AMH (5.0×10^{-5} M) in water; (B) decay dynamics at 470 nm, $\chi^2 = 0.82$. The inset shows the magnified transient absorption from 350 to 400 nm.

~470 nm is assigned to the absorption from the S_0 state of the *trans*-keto tautomer, corresponding well to the time-dependent UV/vis absorption spectra (Fig. S5) and previous reports on photochromic Schiff base [27,28]; thirdly, the positive band with a maximum at ~370 nm is possibly related to a very long-living species, i.e., the *syn*-enol form [3]. This possibility is further confirmed by theoretical calculation (see details and Scheme S1 in the Supporting information). The ground-state absorption of this tautomer partially superimposes with that of the initial *anti*-enol form, accounting for the less negative intensity for the transient absorption in the shorter wavelength range ($\lambda < 360$ nm). Moreover, the transient absorption spectra of AMH in water solution with and without oxygen have been studied, respectively (see Fig. S6 and associated discussion), indicating that the decay of the band does not come from the triplet state. The kinetics of transient signals at 470 nm is shown in Fig. 5B. As the signal observed was very weak, it is necessary to average it over a wide spectral range (445–500 nm) around its maximum in order to reduce the fitting error (Fig. S7) [21]. The decay of the photochrome lifetime is about ~23 μs in water.

3.4. Optical properties of the AMH/PS-LDH films

The fluorescence emission spectra for the AMH/PS-LDH films with different molar ratios of AMH/PS are shown in Fig. 6. When $x \leqslant 10$, the fluorescence intensity at $\lambda = 418$ nm increases at first to a maximum ($x = 2$), then decreases along with a little bathochromic effect until $x = 10$. In the case of $x \geqslant 20$, the maximum emission peak (Fig. 6B) shifts to longer wavelength ($\lambda = 493$ nm), and the fluorescence intensity decreases dramatically as the x value increases. The optimal luminous intensity presents in the sample of 2% AMH-LDH film with the emission peak at 418 nm (the same as pristine AMH in water solution). The red-shift of maximum emission band to 493 nm and its decreasing intensity with $x \geqslant 20$ can be attributed to the change in the state of interlayer AMH anions. The AMH exhibits a single molecular luminescence with low concentration, accounting for the increase in the luminous intensity at first. The J-type aggregates come into formation as AMH increases to a certain concentration, resulting in the red-shift of emission spectra and the fluorescence quenching. Generally, the red-shift indicates stronger intermolecular interactions (especially π–π interaction), resulting from more ordered and dense packing of AMH molecules in the confined region of LDH gallery.

The fluorescence lifetimes of the AMH/PS-LDH ($x = 2$, 10, 50, 75 and 100) samples were measured under the same conditions as solution sample mentioned above, see Fig. S8. The double-exponential decay curves were used in the film samples, which were usually observed in highly heterogeneous environment for the molecules in the solid surfaces [29–31]. As shown in Table 1, the fluorescence lifetime of AMH/PS-LDH (x %) decreases significantly as x increases from 2 to 100, due to the formation of aggregation as indicated by the results of fluorescence spectra. As a result, the longest fluorescence lifetime obtained by two-exponential fitting is presented for the sample of 2% AMH-LDH thin film. Ray et al. suggested that two lifetime values can be attributed to the monomer and dimer or higher aggregates, respectively, in the study of incorporation of sulforhodamine B in the octadecylamine Langmuir–Blodgett (LB) films [32]. In this work, the very short lifetime (*ca.* 1–3 ns) listed in Table 1 may correspond to small amount adsorbed AMH at the surface of LDH particles or the aggregates of AMH in AMH/PS-LDH, especially for the sample with high content of AMH; the long lifetime possibly corresponds to the intercalated monomer AMH in the gallery of LDH, since the interlayer AMH molecule confined between the inorganic sheets is more stably immobilized.

Furthermore, it was found that the fluorescence lifetime of AMH/PS-LDH thin films is much longer than that of AMH in aqueous solution (2.61 ns). The long lifetime possibly originates from the decrease in internal mobility, flexibility and the internal conversion processes of AMH due to the hydrogen bonding and electrostatic interaction between AMH and LDH layers. Meanwhile, the introduction of PS surfactant in the galleries of LDH enhances the emission efficiency of AMH to some extent. Ogawa and Kuroda [33] reported that surfactants or organic solvents can alter the aggregation of photoactive species. In this work, the intercalated surfactant achieves a weak polar interlayer environment, which homogenously dilutes and effectively isolates the interlayer AMH anions.

3.5. Photochromism properties of the AMH/PS-LDH films

The microsecond transient absorption permits a study of the photochromic process and the lifetime of the photochromic tran-

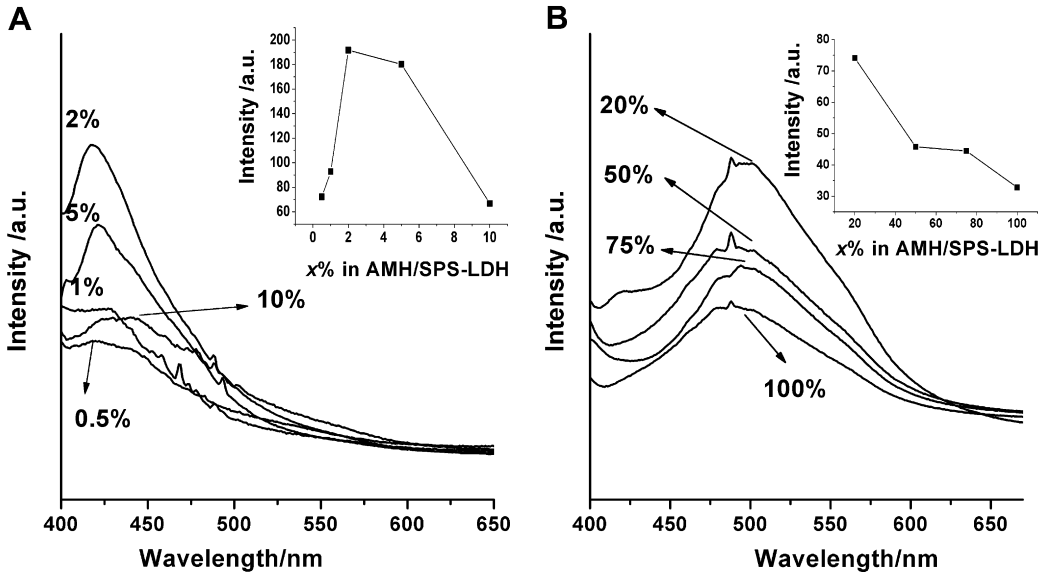

Fig. 6. (A) The photoemission spectra of AMH/PS-LDH films with the excitation wavelength of 360 nm, $x = 0.5$, 1, 2, 5 and 10. (B) The photoemission spectra of AMH/PS-LDH films, $x = 20$, 50, 75 and 100. (Inset: the fluorescence intensity varying with x % in the AMH/PS-LDH films.)

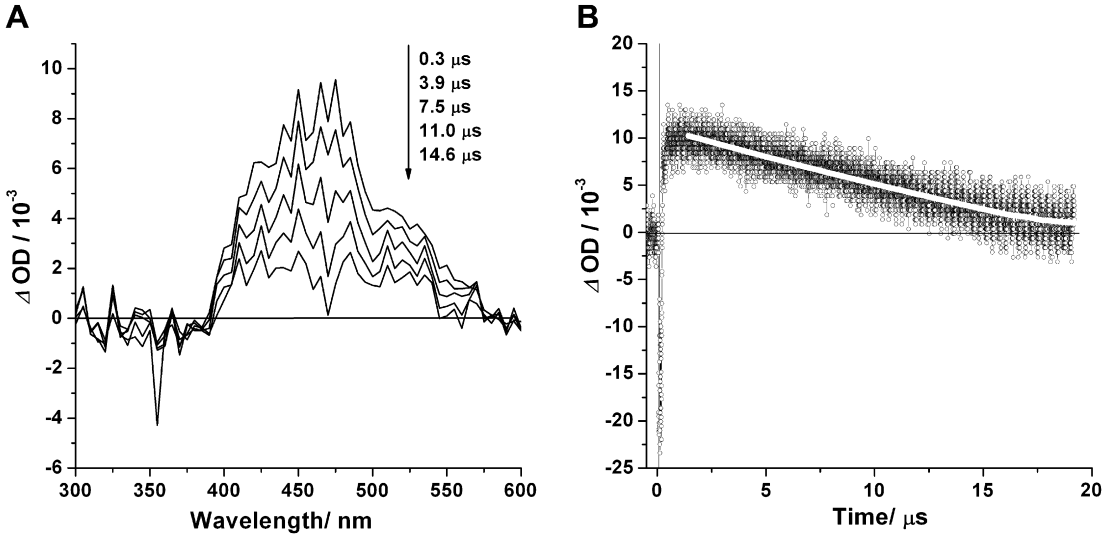

Fig. 7. (A) Transient absorption spectra obtained by laser photolysis for the 2% AMH-LDH film; (B) decay dynamics at 465 nm, $\chi^2 = 0.78$.

sient (*trans*-keto tautomer) of the AMH/PS-LDH films at room temperature. Upon UV excitation, the initial AMH stable as an enol tautomer undergoes an excited-state intramolecular proton transfer to the *trans*-keto tautomer; then the relaxed back-isomerization to the ground state was recorded by transient UV–vis spectroscopy. Fig. 7A shows the transient absorption spectra of the 2% AMH-LDH film after laser flash photolysis at 355 nm. The sharp negative band at 355 nm is due to the scattering of the pump pulse at this wavelength. Besides, the weak negative band centered at 355 nm in the transient absorption spectra is attributed to the ground state absorbance of the enol tautomer, and the absorption band of excited state centered at 465 nm is assigned to the S_0 state of the *trans*-keto tautomer. After intercalation into LDH matrix, the absorption band of excited state for the *trans*-keto tautomer shows a blue-shift of 5 nm compared with pristine AMH molecule, owing to the weak polar micro-environment provided by surrounding PS anions. Furthermore, the decay of the *syn*-enol form was not detected, suggesting that the *syn*-enol/*anti*-enol isomerization was inhibited in the 2D confined environment. As a result, only the photochromic *trans*-keno tautomer in the ground state was observed. The lifetime of *trans*-keto tautomer in 2% AMH-LDH film was obtained by averaging the fit results performed for several observation wavelengths, as shown in Fig. S9. The monoexponential decay curve was applied for the film sample (Fig. 7B and Fig. S9), and the lifetime was calculated to be ~13 μs, which is shorter than that of pristine AMH in water. The lifetime of *trans*-keto tautomer decreases slightly upon incorporation into the LDH matrix, indicating that the *trans*-keto tautomer of AMH is less stable in the 2D confined environment.

4. Conclusions

In summary, AMH and PS were co-intercalated between sheets of ZnAl LDH by the SNAS method, and thin films of AMH/PS-LDH with a well *c*-orientation verified by XRD and SEM, were obtained on quartz substrates by the solvent evaporation method. The optimal luminous sample of AMH/PS-LDH film with 2% AMH molar percentage was obtained for the improvement of the luminescence intensity and lifetime. Compared with the aqueous solution of AMH, the fluorescence lifetime of AMH/PS-LDH films increases greatly (16.69–12.20 ns *vs.* 2.61 ns), due to the immobilization of AMH molecule within the layered matrix. The photochromic cycles of AMH before and after intercalation were investigated by means of the steady state and transient UV–vis spectroscopy. The lifetime of *trans*-keto tautomer in the 2% AMH-LDH film is shorter than that of AMH solution, indicating the *trans*-keto tautomer of AMH is less stable in the 2D confined environment and the ground state of the initial enol tautomer is stabilized in the LDH gallery. The results in this work demonstrate a facile and feasible method for the preparation of photochromic film materials by co-intercalation of chromophore and dispersant into an inorganic 2D host matrix, which can be potentially applied in the field of photoelectronic devices.

Acknowledgments

This project was supported by the National Natural Science Foundation of China, the 111 Project (Grant No. B07004), the 973 Program (Grant No. 2009CB939802) and the Fundamental Research Funds for the Central Universities (Grant No. ZZ0908).

Appendix A. Supplementary data

Supplementary data associated with this article can be found, in the online version, at doi:10.1016/j.cplett.2010.05.071.

References

[1] M. Irie, Chem. Rev. 100 (2000) 1683.
[2] R.V. Andes, D.M. Manikowski, Appl. Opt. 7 (1968) 1179.
[3] M. Ziółek, G. Burdziński, J. Karolczak, J. Phys. Chem. A 113 (2009) 2854.
[4] J. Harada, H. Uekusa, Y. Ohashi, J. Am. Chem. Soc. 121 (1999) 5809.
[5] O.K. Abou-Zied, R. Jimenez, F.E. Romesberg, J. Am. Chem. Soc. 123 (2001) 4613.
[6] F.M. Raymo, S. Giordani, Proc. Natl. Acad. Sci. USA 99 (2002) 4941.
[7] M. Ziółek, K. Filipczak, A. Maciejewski, Chem. Phys. Lett. 464 (2008) 181.
[8] F. Leroux, C. Taviot-Guého, J. Mater. Chem. 15 (2005) 3628.
[9] G.R. Williams, D. O'Hare, J. Mater. Chem. 16 (2006) 3065.
[10] H. Li, J. Ma, D.G. Evans, T. Zhou, F. Li, X. Duan, Chem. Mater. 18 (2006) 4405.
[11] Z. Liu, R. Ma, Y. Ebina, N. Iyi, K. Takada, T. Sasaki, Langmuir 23 (2007) 861.
[12] V. Rives, Layered Double Hydroxides: Present and Future, Nova Science Publishers, New York, 2001.
[13] F. Leroux, J.-P. Besse, F. Wypych, K.G. Satyanarayana, Clay Surfaces: Fundamentals and Applications, Elsevier, London, 2004.
[14] A.M. Fogg, G.R. Williams, R. Chester, D. O'Hare, J. Mater. Chem. 14 (2004) 2369.
[15] L. Li, R.Z. Ma, Y. Ebina, N. Iyi, T. Sasaki, Chem. Mater. 17 (2005) 4386.
[16] L. Mohanambe, S. Vasudevan, Langmuir 21 (2005) 10735.
[17] Y. Zhao, F. Li, R. Zhang, D.G. Evans, X. Duan, Chem. Mater. 14 (2002) 4286.
[18] L.Y. Wang, C. Li, M. Liu, D.G. Evans, X. Duan, Chem. Commun. (2007) 123.
[19] T. Hasegawa, L. Matsumoto, S. Kitamura, S. Amino, S.K. Nishijo, J. Anal. Chem. 74 (2002) 6049.
[20] M. Sliwa, A. Spangenberg, I. Malfant, P.G. Lacroix, R. Métivier, R.B. Pansu, K. Nakatani, Chem. Mater. 20 (2008) 4062.

[21] P. Fita, E. Luzina, T. Dziembowska, D. Kopeć, P. Piątkowski, Cz. Radzewicz, A. Grabowska, Chem. Phys. Lett. 416 (2005) 305.
[22] M. Ziółek, G. Burdziński, K. Filipczak, J. Karolczak, A. Maciejewski, Phys. Chem. Chem. Phys. 10 (2008) 1304.
[23] M. Ziółek, J. Kubicki, A. Maciejewski, R. Naskręcki, A. Grabowska, J. Chem. Phys. 124 (2006) 124518.
[24] T. Sekikawa, T. Kobayashi, T. Inabe, J. Phys. Chem. B 101 (1997) 10645.
[25] M. Sliwa et al., Chem. Mater. 17 (2005) 4727.
[26] Z. Liang, Z. Liu, Y. Gao, Spectrochim. Acta Pt. A 68 (2007) 1231.
[27] S. Mitra, N. Tamai, Chem. Phys. Lett. 282 (1998) 391.
[28] M. Ziółek, J. Kubicki, A. Maciejewski, R. NaskrJcki, A. Grabowska, Phys. Chem. Chem. Phys. 6 (2004) 4682.
[29] K. Rurack, K. Hoffman, W. Al-Soufi, U. Resch-Genger, J. Phys. Chem. B 106 (2002) 9744.
[30] G.P. Wiederrecht, G. Sandi, K.A. Carrado, S. Seifert, Chem. Mater. 13 (2001) 4233.
[31] L. Latterini, M. Nocchetti, G.G. Aloisi, U. Costantino, F.C.D. Schryver, F. Elisei, Langmuir 23 (2007) 12337.
[32] K. Ray, H. Nakahara, J. Phys. Chem. B 106 (2002) 92.
[33] M. Ogawa, K. Kuroda, Chem. Rev. 95 (1995) 399.